epithelial sheet in numerous locations during dorsal closure and followed the subsequent rate of closure with time-lapse confocal microscopy. Surprisingly, the authors observed that no single site of dissection prevented closure. This is probably because the forces that drive closure are distributed among several tissues. In the present work, Toyama *et al*. add the power of genetics to alternatively block programmed cell death or stimulate high levels of cell death specifically in the amnioserosa, and find that dorsal closure is delayed or precocious, respectively.

To quantify the contribution of apoptosis to the vector sum, Toyama *et al*. present a descriptive physics of dorsal closure. The authors surmised that forces are transmitted within and between the amnioserosa and dorsal epidermis through cell-cell junctions along the outer surface of epithelial sheet. Ablating a single cell-cell junction (with a laser) releases the tension locally, and neighboring cells recoil to a new mechanical equilibrium. By following the velocity of newly freed cell-cell junctions, the authors deduced higher tension within the epithelium in embryos with high rates of apoptosis and low tension when cell deaths are blocked.

The occurrence of apoptosis during dorsal closure was discovered nearly 15 years ago (*1*), but its role has not been understood. The simplest explanation was that cell death contributes to dorsal closure by removing surface area from the amnioserosa. However, apoptosis removes only around 10% of the amnioserosa (the rest is resorbed after the epidermis has sealed over it). Alternatively, apoptosis might trigger contraction in other cells that would increase tension within the epithelium and promote cell movement. But strong evidence for this hypothesis is still lacking.

Toyama *et al*. suggest that additional contractive forces may be generated by the neighbors of the dying cell, as they actively excise the dying cell from the amnioserosa. Activation of apical contraction in neighboring cells plays a major role in the excision of cells undergoing apoptosis (*10*) and in the removal of laser-ablated cells (*11*) from epithelial sheets. The spreading of contraction-activation could greatly increase force generation to include neighbors of each apoptotic cell. But why must the contraction-activation signal stop there? Just as forces equilibrate quickly in the epithelium, it seems equally likely that contraction-activation of cell apical surfaces may spread through the entire amnioserosa triggered by even sparse and infrequent dying cells. Such a trigger may resolve another paradox—that the magnitude and spatiotemporal pattern of apoptosis in the amnioserosa vary greatly from embryo to embryo, suggesting that simple removal of dying cells may not be a particularly robust mechanism for ensuring dorsal closure. By serving as a trigger, apoptosis could amplify the contractile efforts to include larger numbers of cells in the amnioserosa.

The coincidence of cell death and epithelial morphogenesis is striking and prompts a rethinking of the role of programmed cell death during morphogenesis. It has been 10 years since the basic intracellular pathways that lead to apoptosis during development were elaborated (*12*), yet the triggers and downstream effectors of apoptotic signals are just beginning to be understood (*13*). Clearly, apoptosis initiates dynamic remodeling of the cytoskeleton (*14*). Whether forces generated during apoptosis contribute to vertebrate morphogenesis remains to be seen, but its ubiquity (*15*) suggests widespread implications and the need for further studies.

References

1. J. M. Abrams, K. White, L. I. Fessler, H. Steller, *Development* **117**, 29 (1993).
2. K. White *et al.*, *Science* **264**, 677 (1994).
3. Y. Toyama, X. G. Peralta, A. R. Wells, D. P. Kiehart, G. S. Edwards, *Science* **321**, 1683 (2008).
4. M. S. Hutson *et al.*, *Science* **300**, 145 (2003).
5. C. Bertet, L. Sulak, T. Lecuit, *Nature* **429**, 667 (2004).
6. J. T. Blankenship, S. T. Backovic, J. S. Sanny, O. Weitz, J. A. Zallen, *Dev. Cell* **11**, 459 (2006).
7. J. Kafer, T. Hayashi, A. F. Maree, R. W. Carthew, F. Graner, *Proc. Natl. Acad. Sci. U.S.A.* **104**, 18549 (2007).
8. M. C. Gibson, A. B. Patel, R. Nagpal, N. Perrimon, *Nature* **442**, 1038 (2006).
9. R. Farhadifar, J. C. Roper, B. Aigouy, S. Eaton, F. Julicher, *Curr. Biol.* **17**, 2095 (2007).
10. J. Rosenblatt, M. C. Raff, L. P. Cramer, *Curr. Biol.* **11**, 1847 (2001).
11. M. Tamada, T. D. Perez, W. J. Nelson, M. P. Sheetz, *J. Cell Biol.* **176**, 27 (2007).
12. M. D. Jacobson, M. Weil, M. C. Raff, *Cell* **88**, 347 (1997).
13. H. Steller, *Cell Death Differ.* **15**, 1132 (2008).
14. O. Ndozangue-Touriguine, J. Hamelin, J. Breard, *Biochem. Pharmacol.* **76**, 11 (2008).
15. A. Glucksmann, *Biol. Rev.* **26**, 59 (1951).

10.1126/science.1164583

CLIMATE CHANGE

Illuminating the Modern Dance of Climate and CO_2

Peter Cox[1] and Chris Jones[2]

Records of Earth's past climate imply higher atmospheric carbon dioxide concentrations in the future.

Climate and atmospheric carbon dioxide (CO_2) concentrations have been coupled through much of Earth's history: CO_2 influences climate through the greenhouse effect, but climate also influences CO_2 through its impact on the stores of carbon on the land and in the oceans. This two-way coupling between climate and CO_2 will have a large influence on how the climate changes over the course of the 21st century. Currently, the amount of CO_2 emitted as a result of human activities is about double the amount required to explain the rate of increase of atmospheric CO_2 (*1*). The remainder is absorbed by land and ocean carbon sinks, which have thus been acting to slow climate change. Will they continue to do so? Data on the Earth's past can illuminate this modern dance of climate and CO_2.

First-generation coupled climate-carbon cycle models (C-CC models) suggest that the ocean and especially land sinks will become progressively less efficient at absorbing CO_2 under global warming (*2*). All such models in the Intergovernmental Panel on Climate Change (IPCC) 4th Assessment Report project higher atmospheric CO_2 by 2100 once the impacts of climate change on the carbon cycle are accounted for (*1*). All models produce increasing carbon sinks as a result of increasing atmospheric CO_2 concentration, which is partially offset by reducing sinks as a result of climate change. The impacts of climate change on the carbon cycle thus lead to a higher fraction of human CO_2 emissions remaining in the atmosphere, and therefore an acceleration of global warming. However, the amount of extra CO_2 simulated by the models varies by an order of magnitude, from the relatively inconsequential [~30 parts per million by volume (ppmv)] (*3*) to the alarming (~250 ppmv) (*4*). It is critically important to reduce this range of uncertainty in climate-carbon cycle feedbacks, because it leads to large uncertainties in the emissions cuts required to stabilize climate at different CO_2 concentrations (*5*).

[1]School of Engineering, Computing and Mathematics, University of Exeter, Exeter EX4 4QF, UK. [2]Met Office Hadley Centre, Exeter EX1 3PB, UK. E-mail: p.m.cox@exeter.ac.uk, chris.d.jones@metoffice.gov.uk

Why can we not use the 20th-century climate record to determine which C-CC models are likely to be most accurate? Temperature and CO_2 have both increased almost continuously through the 20th century, making it difficult to separate the positive impacts of CO_2 on carbon sinks from the negative impacts of global warming on these sinks. The existing C-CC models can roughly reproduce the 20th-century increase in CO_2 despite having great variations in the relative impacts of CO_2 and climate change on carbon sinks. Models in which both effects are large can reproduce the observational record, but so can models in which both effects are small (see the figure, left panel). However, these different possibilities result in a wide range in the projected CO_2 concentration by 2100 under a given human CO_2 emissions scenario (*2*). We clearly need other observational constraints to tie down the climate-carbon feedback.

Interannual variability in the atmospheric CO_2 concentration is a ubiquitous signal in the observational record that could help us distinguish between different models. The growth rate of atmospheric CO_2 varies from year to year as a result of climatic anomalies associated with the El Niño–Southern Oscillation (*6*) and volcanic eruptions (*7*), and this can be seen in some C-CC general circulation models (GCMs). We find that models with a larger sensitivity of CO_2 growth rate to interannual climate variations also show a stronger climate-carbon feedback. As a result, the observed interannual variability provides an additional observational constraint on the sensitivity of carbon stores to climate (see the horizontal lines in the figure, left panel). However, the relatively small number of C-CC GCMs means that the gradient of this relation is not well constrained, so the overall uncertainty in the extra CO_2 to be expected for each unit of warming is still very large, ranging from 3 to 31 ppmv/K (see description of methods).

How can paleoclimatic data help? The key challenge is to find a period in the past when CO_2 has varied mainly as a result of a natural climate variation with a time scale relevant to 21st-century climate change. The most marked example of coupled variations between climate and CO_2 concerns the glacial-interglacial cycles, but these cycles occur on time scales of 1000 to 100,000 years, and thus involve processes that may not be relevant to century-scale climate change (*8*). By contrast, the Little Ice Age (LIA) perturbation in climate (*9*) and CO_2 (*10*) is much smaller, but has the advantage of having occurred over a time scale of a few centuries.

The perturbations of climate and CO_2 during the LIA period from 1500 to 1750 are strongly correlated, with climate leading CO_2 by ~50 years (*11*). These records indicate a tight relation between CO_2 and climate, with a gradient of 40 ppmv/K. However, given the discrepancies between different temperature reconstructions, and the uncertainties associated with interpreting Northern Hemisphere climate proxies in terms of global mean temperature, we estimate a gradient of 20 to 60 ppmv of CO_2 per kelvin of global warming (see the figure, middle panel).

This is a conservative estimate based on the assumption that human CO_2 emissions from land-use change (*12*) were not significant in the LIA, which seems consistent with the strong lead-lag relationship between climate and CO_2 during this period. Even so, the estimate is at the high end of the 20th-century simulations with the IPCC C-CC models, encompassing only the model with the largest feedback over this period. When considered alongside contemporary constraints, the LIA data thus enable a much tighter constraint on the climate and CO_2 dependences of the carbon cycle (see the figure, right panel).

The LIA data imply that atmospheric CO_2 will increase more quickly with global warming than most models suggest. One implication is that the 20th-century CO_2 rise due to anthropogenic emissions may have been amplified by 20 to 30 ppmv through the impacts of global warming on natural carbon sinks. Furthermore, the existence of a strong climate effect on the carbon cycle indicates that larger emissions cuts are required to stabilize CO_2 concentrations at a given level. The LIA is just one example of a natural climatic anomaly in the past that can provide insights into the strength of the coupling between the Earth's climate and carbon cycle. Paleoclimatic data cannot tell us how to meet the challenge of managing 21st-century climate change, but they can help us to better understand the nature of this challenge.

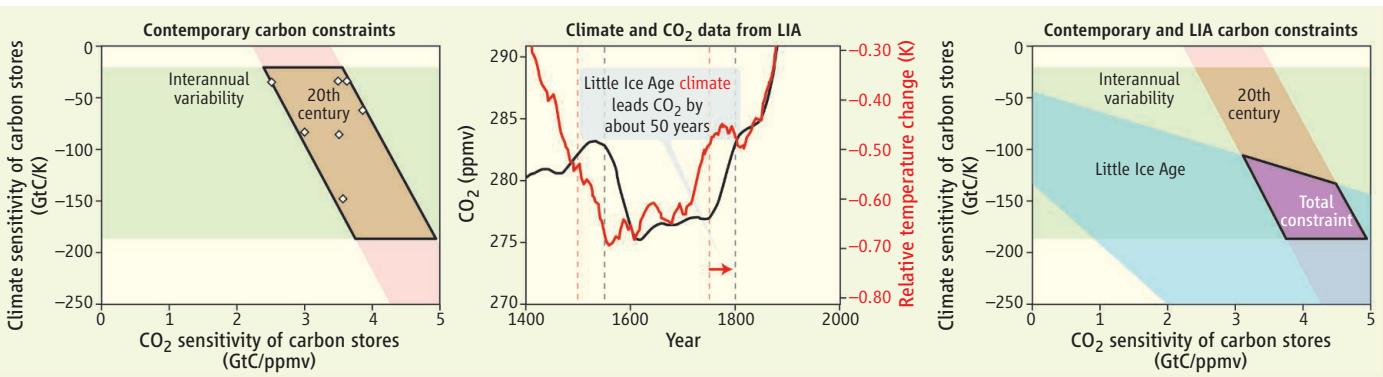

Impact of Little Ice Age (LIA) data on estimates of climate-carbon feedback. (**Left**) Constraints on the climate and CO_2 sensitivities of the carbon cycle based on 20th-century trends (pink) and interannual variability (green). The diagonal band at the top right corner represents the combinations of climate and CO_2 effects on the carbon cycle that are consistent with the 20th-century record. This band has a finite width because of substantial uncertainties in the net land-use emissions of CO_2. As a result, it encompasses the 20th-century simulations of all seven current C-CC GCMs, even though these models predict a wide range of climate-carbon feedbacks for the 21st century. We exclude from this plot the four Earth System Models of Intermediate Complexity (EMIC) reported in (*2*), because these models lack interannual variability. (**Middle**) Variation of climate (red) and CO_2 (black) through the LIA (1500 to 1750) (*9*, *10*). (**Right**) Total constraint on the climate and CO_2 sensitivities of the carbon cycle (purple rhombus) once the LIA constraint is added to the contemporary constraints. Inclusion of the LIA data substantially reduces the overall uncertainty in the carbon cycle responses to both climate and CO_2.

References and Notes

1. K. L. Denman *et al.*, in *Climate Change 2007: The Physical Science Basis. Contribution of Working Group I to the Fourth Assessment Report of the Intergovernmental Panel on Climate Change*, S. Solomon *et al.*, Eds. (Cambridge Univ. Press, Cambridge, UK, 2007), chap. 7.
2. P. Friedlingstein *et al.*, *J. Climate* **19**, 3337 (2006).
3. I. Y. Fung, S. C. Doney, K. Lindsay, J. John. *Proc. Natl. Acad. Sci. U.S.A.* **102**, 11201 (2005).
4. P. M. Cox, R. A. Betts, C. D. Jones, S. A. Spall, I. J.

Totterdell, *Nature* **408**, 184 (2000).
5. C. D. Jones, P. M. Cox, C. Huntingford, *Tellus B* **58**, 603 (2006).
6. C. D. Jones, M. Collins, P. M. Cox, S. A. Spall. *J. Climate* **14**, 4113 (2001).
7. C. D. Jones, P. M. Cox, *Global Biogeochem. Cycles* **15**, 453 (2001).
8. D. Archer, D. Kheshgi, E. Maier-Reimer. *Geophys. Res. Lett.* **24**, 405 (1997).
9. A. Moberg, D. M. Sonechkin, K. Holmgren, N. M. Datsenko, W. Karlen, *Nature* **433**, 613 (2005).
10. D. M. Etheridge *et al.*, *J. Geophys. Res.* **101**, 4115 (1996).
11. M. Scheffer, V. Brovkin, P. M. Cox, *Geophys. Res. Lett.* **33**, L10702, 10.1029/2005GL025044 (2006).
12. W. F. Ruddiman, *Clim. Change* **61**, 261 (2003).
13. This paper is based on a presentation given at the Leverhulme Climate Symposium 2008: "Earth's Climate: Past, Present and Future." We thank the Coupled Climate-Carbon Cycle Model Intercomparison Project (C^4MIP) for providing model outputs for this analysis.

The contribution of C.J. was supported by the Defra and MoD Integrated Climate Programme (Contract number: GA01101, CBC/2B/0417_Annex C5).

Supporting Online Material
www.sciencemag.org/cgi/content/full/321/5896/1642/DC1
Methods
Figs. S1 to S4
References

10.1126/science.1158907

MICROBIOLOGY

Desperately Seeking New Antibiotics

New approaches for discovering the next generation of antibiotics are needed to combat the rise in bacteria that are resistant to current drugs.

David J. Payne

The need for new antibiotics is undisputed (*1*). Recent studies estimate that more people die from the methicillin–resistant *Staphylococcus aureus* (MRSA) bacterium than from HIV in the United States (*2*), and the Centers for Disease Control and Prevention estimates that more than 90,000 people die from hospital-acquired bacterial infections in the United States each year. Numerous reports have illustrated the "perfect storm" of rising bacterial resistance to antibiotics and an industry pipeline ill-equipped to address the need for new antibacterial drugs (*3*, *4*) (see the figure). Consequently, the reports by Haydon *et al.* on page 1673 in this issue (*5*) and by Rasko *et al.* (*6*) are important because they validate and illustrate the therapeutic potential of two new antibacterial drug targets. In addition, the paper by Hiratsuka *et al.* on page 1670 in this issue (*7*) identifies a biosynthetic pathway that may provide new antibacterial strategies for certain species of bacteria.

Haydon *et al.* report the discovery of a class of drugs that targets the bacterial protein FtsZ. FtsZ is related to the human cytoskeletal protein β-tubulin and is essential in bacterial cell division in most Gram-positive and Gram-negative pathogens, where it polymerizes to form a ring at the mid cell that enables septum formation. The authors show by crystallographic analysis that their lead molecule (PC190723) binds to the region of FtsZ that is analogous to the site that the anticancer drug Taxol binds to in β-tubulin (Taxol interferes with microtubule dynamics and blocks cell division). Moreover, they show that PC190723 possesses in vitro potency against MRSA, and is effective in a mouse model of *S. aureus* infection. Importantly, through mutational and bacterial physiology experiments, Haydon *et al.* show that the antibacterial effect of PC190723 is via inhibition of FtsZ. The discovery of these inhibitors of FtsZ illustrates the potential of this protein as a novel and exploitable antibacterial drug target.

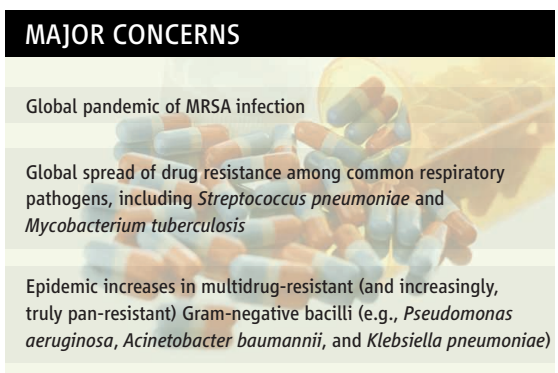

Bad bugs need drugs. Three major areas of concern that need new antibiotics [as defined by the Infectious Diseases Society of America (*4*)].

Whereas inhibition of FtsZ prevents bacterial growth, Rasko *et al.* describe an alternative drug approach that cripples the bacteria's ability to maintain an infection. The authors discovered a compound (LED209) that inhibits the bacterial enzyme QseC. This target is a histidine kinase that autophosphorylates upon sensing either host signaling molecules (the hormones norepinephrine and epinephrine) or bacterial molecules (called autoinducers) associated with quorum-sensing (cell-to-cell communication among bacteria). This phosphorylation event leads to the expression of key virulence genes, and *Escherichia coli* with a mutant form of QseC is unable to trigger expression of these virulence genes and shows decreased growth in an animal infection model. QseC homologs are found in most clinically important Gram-negative pathogens. Rasko *et al.* elegantly demonstrate that LED209 inhibits QseC-dependent expression of virulence genes triggered by either the autoinducer AI-3 or by epinephrine. In animal models of infection, LED209 was not effective in protecting against *E. coli* infection, but oral dosing of LED209 3 hours before and after infection with *Salmonella typhimurium* protected mice from infection. In addition, fewer bacteria were recovered from the spleens and livers of animals treated with LED209 compared with controls. Therefore, this work demonstrates the potential of an "antivirulence" strategy for tackling bacterial infections. None of the currently available antibiotics employ such a mechanism of action.

Hiratsuka *et al.* illustrate the power of bacterial genomics to identify potential new targets for anti-infective strategies. Most microorganisms use a biosynthesis pathway encoded by the *men* genes to produce menaquinone, a molecule needed for bacterial anaerobic respiration. However, the authors deduced that some bacteria such as *Streptomyces coelicolor*, *Helicobacter pylori*, and *Campylobacter jejuni* lack these genes, yet still synthesize menaquinone. To identify this new route of synthesis, the authors compared the genomes of microorganisms that use the known *men* pathway with bacteria that lack the *men* genes. This eventually led to four candidate genes, each of which were previously annotated as encoding "hypothetical proteins." Each of these genes was disrupted, and the resulting mutants all required menaquinone for growth. The authors then used biochemical and analytical approaches to identify the various intermediate molecules at each step in the new menaquinone

Antibacterial Disease Performance Unit, Infectious Diseases Center of Excellence, GlaxoSmithKline, Collegeville, PA 19426, USA. E-mail: david.j.payne@gsk.com